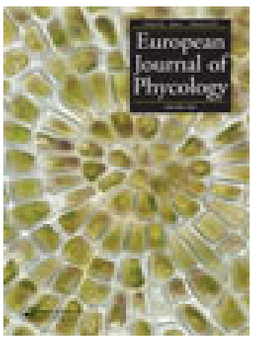

European Journal of Phycology

ISSN: 0967-0262 (Print) 1469-4433 (Online) Journal homepage: http://www.tandfonline.com/loi/tejp20

Rivularia halophila sp. nov. (Nostocales, Cyanobacteria): the first species of *Rivularia* described with the modern polyphasic approach

Sergei Shalygin, Nicole Pietrasiak, Fernando Gomez, Cecilia Mlewski, Emmanuelle Gerard & Jeffrey R. Johansen

To cite this article: Sergei Shalygin, Nicole Pietrasiak, Fernando Gomez, Cecilia Mlewski, Emmanuelle Gerard & Jeffrey R. Johansen (2018): *Rivularia halophila* sp. nov. (Nostocales, Cyanobacteria): the first species of *Rivularia* described with the modern polyphasic approach, European Journal of Phycology

To link to this article: https://doi.org/10.1080/09670262.2018.1479887

EUROPEAN JOURNAL OF PHYCOLOGY, 2018
https://doi.org/10.1080/09670262.2018.1479887

Rivularia halophila sp. nov. (Nostocales, Cyanobacteria): the first species of *Rivularia* described with the modern polyphasic approach

Sergei Shalygin [a,b], Nicole Pietrasiak[a], Fernando Gomez[c], Cecilia Mlewski[c], Emmanuelle Gerard[d] and Jeffrey R. Johansen[b,e]

[a]Department of Plant and Environmental Sciences, New Mexico State University, 945 College Drive, Las Cruces, NM 88003, USA; [b]Department of Biology, John Carroll University, University Heights, OH 44118 USA; [c]LAC-Laboratorio de Análisis de Cuencas, CICTERRA (CONICET-UNC) Centro de Investigaciones en Ciencias de la Tierra, FCEFyN-Universidad Nacional de Córdoba, (Córdoba) Argentina; [d]Genomic laboratory, Institut de Physique du Globe, Paris; [e]Department of Botany, Faculty of Science, University of South Bohemia, Branišovská 31, 370 05 České Budějovice, Czech Republic

ABSTRACT

Natural populations of a *Rivularia*-like cyanobacterium were collected from the carbonate deposits of the temporarily flooded littoral zone of a hypersaline, high elevation lake, The Laguna Negra, Andes, Argentina. Subsequently, the cyanobacterial strain PUNA-NP3, named after its origin (Puna Volcanic Plateau) was isolated from these *Rivularia*-like rounded, pillow-like, black microbial mats. None of the previously described species of the genus *Rivularia* occupy inland, hypersaline aquatic environments. After morphological examination of this strain, we found clear morphological autapomorphies, such as mucilaginous pads at the bases of the young trichomes, wide trichomes and filaments, and uniquely branched trichomes. Furthermore, based on results from 16S rRNA phylogeny and analysis of the 16S-23S ITS region, PUNA-NP3 was found to be an independent lineage of the evolutionary tree. Based on the combination of ecological, morphological and molecular evidence, we name strain PUNA-NP3 *Rivularia halophila* sp. nov. a new species under requirements of the International Code of Nomenclature for Algae, Fungi and Plants.

ARTICLE HISTORY Received 22 December 2017; Revised 6 February 2018; Accepted 10 April 2018

KEYWORDS 16S rRNA gene phylogeny; 16S-23S ITS; Andes Mountains; Cyanobacteria; polyphasic approach; *Rivularia*; *Rivularia halophila*

Introduction

Rivularia is one of the most charismatic genera of the Cyanobacteria. Many species of *Rivularia* form beautiful, blue-green spherical and hemispherical macroscopic colonies that can grow up to several centimetres across in their natural habitats, making recognition of *Rivularia* easy even in field material. Despite this, it is not often reported in floristic surveys because of its rare occurrence (Shalygin, 2012; Davydov, 2017; Vondrášková *et al.*, 2017). *Rivularia* spp. occupy diverse ecological niches, including freshwater, marine and terrestrial habitats (Hindák, 2007; Komárek, 2013; Berrendero Gómez *et al.*, 2016). In aquatic ecosystems, some *Rivularia* species are capable of precipitating calcium carbonate inside their mucilage (Obenlüneschloss & Schneider, 1991). Subsequently, calcium carbonate crystals among the filaments can fossilize, informing palaeoecological reconstructions of palaeoclimate (Golubic, 1973; Golubic & Campbell, 1981; Pentecost, 1988; Brandes *et al.*, 2015). Other members of this genus may serve as bioindicators of current environmental conditions in marine, brackish or freshwater ecosystems (Perona & Mateo, 2006). This is mainly due to the fact that *Rivularia* spp. are often confined within strict physical and chemical limits, such as salinity levels (Oren, 2015).

Excluding inadequately described and unclear taxa, the genus *Rivularia* contains 33 species, consisting of 20 freshwater, 10 marine and three terrestrial species (Komárek, 2013). It belongs to the family Rivulariaceae, together with *Isactis*, *Calothrix*, *Dichothrix*, *Kyrtuthrix*, *Gardnerula*, *Sacconema* and *Nunduva* (Komárek, 2013; León-Tejera *et al.*, 2016; González-Resendiz *et al.*, 2018). All members of this family are characterized by having unbranched or falsely branched heteropolar tapering filaments (Komárek, 2013). Historically, the family Rivulariaceae united a number of heterocytous taxa including *Calothrix* and *Rivularia* as well as non-heterocytous genera, such as *Homoeothrix* (Bornet & Flahault, 1888). After Geitler's revision, Rivulariaceae still had one non-heterocytous genus, *Raphidiopsis* (Geitler, 1932). Subsequently, Elenkin (1938) removed all taxa without heterocytes from the Rivulariaceae, and limited the family to three major genera: *Calothrix* (with *Dichothrix* as a subsection), *Rivularia* (with *Isactis*) and *Gloeotrichia*. Recently, several authors have studied various representatives of the Rivulariaceae using molecular DNA-based tools and found the family to be polyphyletic (Sihvonen *et al.*, 2007; Domínguez-Escobar *et al.*, 2011; Berrendero Gómez *et al.*, 2016). The family still contains the genus

CONTACT Sergei Shalygin sshalygin18@jcu.edu

Published online 05 Oct 2018

Calothrix, which forms a clade paraphyletic to *Rivularia* based on molecular evidence; the Calothrichaceae should be named, typified and separated from Rivulariaceae (Komárek *et al.*, 2014).

With the increasing number of metagenomic studies, it is important to have well-established DNA reference benchmarks for monophyletic genera and species, especially those based on ecological and floristic studies. This has not been accomplished yet for the genus *Rivularia*. Although a number of sequences in NCBI are identified as *Rivularia* sp., we still do not have an established DNA-based phylogenetic benchmark for the type species of the genus, leading to inconsistencies within the literature (Berrendero Gómez *et al.*, 2016; Shalygin *et al.*, 2017). For instance, several authors, such as Komárek (2013), León-Tejera *et al.* (2016), Shalygin *et al.* (2017) and Guiry & Guiry (2017) report *R. dura* Roth *ex* Bornet & Flahault as the type species of the genus, while Berrendero Gómez *et al.* (2016) report *R. atra* Roth *ex* Bornet & Flahault as the type. This confusion arises from the fact that two lectotypifications of *Rivularia* were reported in the first half of the 20th century, *R. atra* by Gardner (1932) and *R. dura* by Geitler (1942). Gardner's lectotypification has priority, despite the common acceptance of *R. dura* as type by later authors.

Herein, using the polyphasic approach including morphology, ecology, 16S rRNA gene and 16S-23S ITS molecular markers, and applying the monophyletic species concept (Johansen & Casamatta, 2005), we describe a new species of *Rivularia, Rivularia halophila*.

Materials and methods

Collection site, cultivation and morphology

Black and white microbial mats were collected from the shallow, temporarily flooded littoral of the hypersaline, alkaline lake, Laguna Negra, Andes, Puna Volcanic Plateau, Argentina (27°38′49″S, 68° 32′43″W, altitude ~4110 m). The Laguna Negra is a shallow, 8.63 km^2 hypersaline lake (Fig. 1) with salinity as high as 120 ‰, and it is subject to extreme environmental conditions, such as high UV influx, strong winds and a stable negative hydrological balance (Gomez *et al.*, 2014).

Rivularia halophila PUNA-NP3 was isolated from a black mucilaginous mat which contained the species of interest mixed with other algae and bacteria. Isolation was achieved by serial picking and rinsing of the heterocytous filaments with a Pasteur pipette, then placing them onto enriched Petri plates with agar Z8 medium (Kotai, 1972). After ~2 years of cultivation at room temperature (25°C) and in a growth chamber (16°C) with 12:12 hours light:dark regime with moderate growth, we transferred the strain into marine F/2 media (Guillard & Ryther, 1962). We used nitrogen-free Z8 medium to induce heterocyte production. Images of life stages were obtained with a Zeiss Axioscope photomicroscope with DIC optics (Zeiss, Oberkochen, Germany). All morphometric characteristics, such as width of trichomes and filaments, were measured in Zeiss AxioVision LE software (Zeiss, Oberkochen, Germany). To document morphological information from the natural habitat of the new species of *Rivularia*, we used Confocal Laser Scanning Microscopy (CLSM) imaging. Embedded and formaldehyde-fixed microbial mat samples were examined at the Institut de Physique du Globe de Paris using a FluoViewTM FV1000 confocal laser scanning microscope with a spectral resolution of 2 nm and a spatial resolution of 0.2 µm (Olympus Corp., Tokyo, Japan). The FluoViewTM 10 FV1000 was equipped with a 405 nm laser diode, and multi-line argon (458 nm, 488 nm and 515 nm), helium-neon-green (543 nm) and helium-neon-red (633 nm) lasers. Fluorescence images were obtained with concomitant excitation at wavelengths of 405 nm, 488 nm and 543 nm by collecting the emitted fluorescence between 425–475 nm, 500–530 nm and 560–660 nm, respectively. For CSLM image acquisitions of embedding slices, a water immersion LUMPLFL 60XW objective (Olympus; 60× magnification) with numerical aperture (N.A.) of 0.9 was used. 3D images were acquired, visualized and processed using the F10-ASW FLUOVIEW software (Gérard *et al.*, 2013).

Culture material of *R. halophila* was deposited in: the John Carroll University Culture Collection (JCUCC), accession number JC6838; the New Mexico State University Culture Collection (NMSUCC), reference strain number *R. halophila* PUNA-NP3; the National Center for Marine Algae and Microbiota (NCMA), accession number CCMP 3497; and the Culture Collection for Autotrophic Organisms (CCALA), as CCALA 1120. Holotype material was prepared as dried biomass and also preserved in a 4% formaldehyde solution, and deposited into the NMSU herbarium, with accession number NMC865010. Additionally, comprehensive graphical and text information about *R. halophila* was shared on the internet using CYANOpro, under a Creative Commons License (Melechin *et al.*, 2013).

Molecular methods

DNA was extracted from culture material using a phenol:chloroform:isoamyl alcohol method according to the procedure described in Countway *et al.* (2005). Polymerase chain reaction (PCR) of the 16S rRNA gene and associated 16S-23S ITS region was performed following Perkerson *et al.* (2011). Amplicons were cloned in order to better recover the ITS regions of multiple operons (Johansen *et al.*, 2017) and sent to Functional Biosciences, Inc. (Madison, Wisconsin,

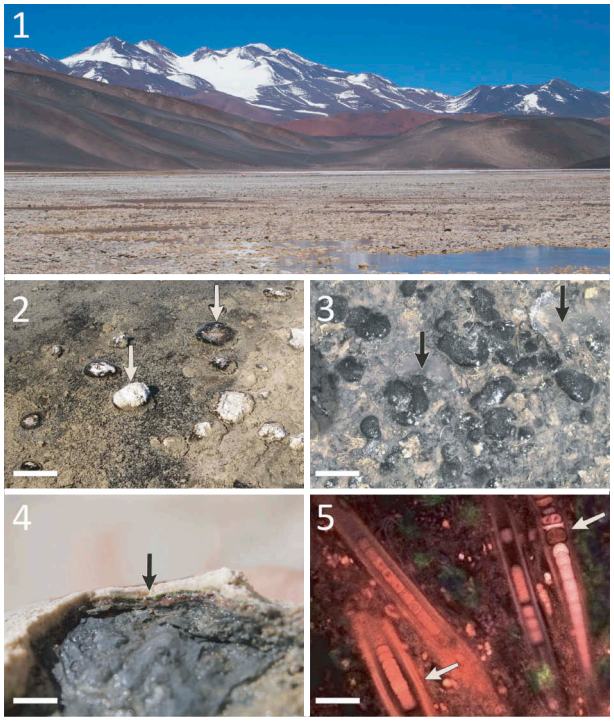

Figs 1–5. Photographs and micrograph of *Rivularia halophila* from the type locality. **Fig. 1**. Habitat. **Fig. 2**. Free living (black) and encrusted (white) macrocolonies, indicated with arrows. **Fig. 3**. Young, hemispherical and rounded macrocolonies; note transparent salt crystals, indicated by arrow. **Fig. 4**. Cross-section of the macrocolony with calcium precipitation, indicated with arrow. **Fig. 5**. Confocal micrograph of the robustly enveloped individual trichomes, indicated with arrow, the one on the right side bearing an intercalary heterocyte (arrow) with paraheterocytic necridia. Scale bars: Fig. 2 = 10 cm, Fig. 3 = 2 cm, Fig. 4 = 1 cm, Fig. 5 = 20 µm.

USA) for sequencing. The sequence was submitted to NCBI and assigned to the following accession number: KY296608 (Shalygin *et al.*, 2017).

Phylogenetic analyses

For the phylogenetic analyses, sequences of the 16S rRNA gene were collected from NCBI before 1 March 2017. We aimed to add as many new taxa from Nostocales as possible. If two sequences in the terminal clade were 100% identical, one of them was removed from the data matrix. Short sequences (<700 bp) were excluded from the analysis (Yarza *et al.*, 2014). In the end, around two-thirds of all sequences from our data matrix were *c.* 1500 bp long, while one-third were *c.* 1200 bp long, allowing us to capture the highly variable but phylogenetically informative V9 region of the 16S rRNA gene, also known as H44 (Řeháková *et al.*, 2014; Yarza *et al.*, 2014). After aligning the sequence matrix in Mega 7.0. using Muscle (Kumar *et al.*, 2016) we manually aligned the V9 region according to the secondary structure of the rRNA molecule (Řeháková *et al.*, 2014).

GTR+I+G was estimated as the best model by the jModeltest2 software (Darriba *et al.*, 2012), and subsequently used for BI and for ML. BI, ML and jModeltest2 runs were calculated using a supercomputer on the CIPRES science gateway (Miller *et al.*, 2015). MrBayes v. 3.2.6 (Ronquist *et al.*, 2012) was used for BI, with two runs of eight Markov chains, with 40 million generations, sampling every 100 generations, applying a 25% burn-in. We used the sump command to stop analysis after Markov chains merged. The BI analysis had a mean estimated sample size (ESS) exceeding 400 for all parameters (range 483–19 325), well above the average of 200 typically accepted as sufficient by phylogeneticists (Drummond *et al.*, 2006). The final average standard deviation of split frequencies was 0.0100. The potential scale reduction factor (PSRF) value for all the estimated parameters in the Bayesian analysis was 1.00, indicating that convergence of the MCMC chains was statistically achieved (Gelman & Rubin, 1992). For ML analysis, RaxML v. 7.2.8 (Stamatakis *et al.*, 2008) was used with 1000 bootstrap replicates. Maximum parsimony (MP) analysis was accomplished using PAUP v. 4.02b (Swofford, 2002). Bootstrap analyses were performed with heuristic searches using 1000 bootstrap replicates.

P-distance values for ITS region were calculated using Mega 7.0 (Kumar *et al.*, 2016) according to the ITS alignment created in Geneious R10 (Kearse *et al.*, 2012). Secondary structures of the ITS region were predicted based on sequence regions flanked by the conserved basal clamp regions of the major helices, which in cyanobacteria are 5′–GACCU:AGGUC–3′ for the D1-D1′ helix and 5′–AGCA:UGCU–3′ for the Box-B helix. The V2 helix, when present, is defined by its position between the two tRNA genes. The V3 helix is identified by position, following the Box-A (consensus 5′–GAACCTTGAAA–3′) and attached D4 region (18–22 nucleotides after Box-A). The V3 helix has variable clamp sequences. Once putative folding regions were found in the sequence, they were folded with Mfold using the untangle with loop fix option for structure draw mode, with other parameters set at default (Zuker, 2003). Structures were then redrawn and colour coded in Adobe Illustrator CC (Adobe Systems Inc., San Jose, California, USA).

Results

Rivularia halophila Shalygin & Pietrasiak, sp. nov. (Figs 1–17, Supplementary figs S1–12)

DIAGNOSIS: Differing ecologically from all described species by occurrence in hypersaline evaporation lake. Similar to calcified species *R. haematites*, *R. dura* and *R. rufescens*, but having basal cells distinctly shorter than wide with greater maximal width. Also similar to *R. biasolettiana*, from which it differs by presence of

Table 1. Phenetic and biogeographic comparison of *Rivularia halophila* with some more or less morphologically similar taxa. Most informative morphological and ecological characteristics were chosen for comparison analysis. Information gathered from Komárek (2013) and Dillon *et al.* (2003).

	R. halophila	'*Calothrix*' sp. CCMEE5093	*R. atra*	*R. dura*	*R. biasolettiana*	*R. haematites*
Substrate	**Flooded carbonate deposits**	Siliceous deposits	Stones, seaweeds	Submersed water plants	Stones, submersed water plants	Stones
Ecology	**Hypersaline**	Thermal springs with temperature range 20–35 °C	Marine/brackish	Freshwater	Freshwater/high salinity	Calcareous waters
Location	**Argentina/Andes**	Yellowstone National Park (USA)	North temperate	Cosmopolitan/ Argentina	North temperate	North temperate
Calcium precipitation	+	–	–	+	+	+
Macrocolony	**Spherical/ Hemispherical**	Maximum a 3 layered prostrate mat	Spherical/ Hemispherical	Hemispherical	Spherical/ Hemispherical	Hemispherical/ Irregular
Filament width	**7–20 (35) µm**	8–12 µm	not reported	15.5–20 µm	10–30 µm (18 µm maximum from original description)	not reported
Cell width at base	**7–17 µm**	not reported	2–6 µm	4–9 µm	3–13 µm	3–11 µm
Sheath	**Lamellated, brown, colourless in culture, collars not observed**	Lamellated, yellow, collars	Lamellated, yellowish, collars	Lamellated, yellowish, collars	Lamellated, yellow-brown, collars	Lamellated, colourless, with collars

granules inside the cells, presence of slime pads, branching pattern and geographic distribution (Table 1).

DESCRIPTION: In the natural environment, blackish macroscopic colonies compact, irregular-spherical to hemispherical, sometimes pillow-like, attached to the substrate, establishing microbial communities with eukaryotic algae and heterotrophic bacteria, often encrusted and surficially whitened with calcium carbonate, up to several cm. Filaments initially short, long in older stages, both commonly singly and geminately branched, with young isopolar *Tapinothrix clintonii*-like forms with trichomes tapered towards both ends, usually attached to the long, lamellated main filaments, maximally 500 µm long. Young filaments isopolar or heteropolar, sometimes with geminate branches, rarely aggregated into star-like fascicles (up to 20 µm in diameter), occasionally attached to long main filaments. Sheaths firm, attached to trichomes or widened, usually intensely lamellated, sometimes with perpendicular striations near branches, rarely swollen, usually colourless, yellowish when old or slightly violet, up to 35 µm wide. Mucilaginous pads on the surface of the sheaths of the main filaments connecting those with the young attenuated trichomes. Trichomes usually single, sometimes two inside a single widened sheath, attenuated, rarely with moderately long hairs, 7–12 (17) µm wide. In senescent cultures, long trichomes not or slightly constricted at crosswalls, sometimes coiled inside the thick, robust sheath, 8–17 (19) µm wide. Meristematic zones present with densely packed short cells. Cells near the bases usually distinctly shorter than wide, rarely up to isodiametric, in hairs (when present) always longer than wide, barrel-shaped when young, rarely almost without constrictions in old filaments, granulated, intensely blue-green, sometimes with several small or a few massive granules, in short trichomes very constricted, with sub-spherical cells, dividing by centripetal binary fission. Heterocytes rare in nitrogen-rich media, in nitrogen-free medium heterocytes of different shapes and sizes, intercalary and terminal, occasionally two in a row, 10–12 (19) µm in diameter. Necridic cells with colour similar to vegetative cells, but sometimes brown. Reproducing by short, 2–8 (12) celled hormogonia, tapered to one end or isopolar, rarely with a basal heterocyte.

TAXONOMIC NOTES: In Z8 and F/2 culture media, macroscopic colonies blue-green, spreading from the centre, forming more or less flat (on solid Z8 medium) as well as rounded *Rivularia*-like fascicles (in liquid F/2 medium) up to several mm, with visible long, main filaments. Additionally, slightly elongated hairs were observed in F/2 culture material, a characteristic typical of the genus (Komárek, 2013).

Mucilaginous collars were not observed under natural or cultural conditions, although reported in some natural populations of *Rivularia* and shown to precipitate calcium crystals (Golubic & Campbell, 1981; Obenlüneschloss & Schneider, 1991; Merz-Preiß & Riding, 1999). *Rivularia halophila* appears capable of calcium carbonate precipitation inside the mucilaginous sheaths (Figs 2, 4, Table 1), but given the presence of other cyanobacterial species in the mat, we cannot be sure it is *Rivularia* that is the source of the calcification. Efforts are currently underway to physiologically confirm that *R. halophila* is the source of the calcium carbonate precipitation in the laboratory (Fernando Gomez, unpublished).

ETYMOLOGY: named for the occurrence in non-marine hypersaline habitat; *halos* (Gr.) = salt, *phílos* (Gr.) = loving, *halophila* (Gr. fem. adj.) = salt-loving.

HOLOTYPE HERE DESIGNATED: NMC865010, New Mexico State University Herbarium, Las Cruces, New Mexico, as dried biomass and also preserved in 4% formaldehyde solution.

TYPE LOCALITY: Argentina, Catamarca Province, Laguna Negra, 27°38′49″ S, 68°32′43″W, altitude ~4010 m, from temporarily flooded littoral of the lake Laguna Negra (alkaline, hypersaline), situated in hyperarid environment, attached to the substrate, close to the air-water interface among precipitated salt crystals (Figs 1–3).

REFERENCE STRAIN: *Rivularia halophila* PUNA-NP3 deposited in the JCU (JC6838) and NMSU culture collection (PUNA-NP3), also CCALA 1120 and CCMP 3497.

AVAILABLE SEQUENCE: KY296608 (partial 16S rRNA gene with associated complete 16S-23S ITS region).

Differentiation from similar species

Rivularia halophila fits well within the morphological description of the genus *Rivularia*, by having spherical and hemispherical macrocolonies with calcium precipitations in the natural populations, spherical colonies in liquid F/2 media, parallel arrangement of filaments, as well as filaments that taper to hairs (Figs 2–4, Figs 7–8, Supplementary fig. S12). However, *R. halophila* also shows unique autapomorphies, permitting its description as a new species, including: (1) dimensions (trichomes and filaments are wider than most other species of *Rivularia*); (2) appearance of mucilaginous pads at the base of young tapering filaments, connecting to older filaments (Fig. 10); (3) frequent single and geminate false branching of the trichomes in cultured material (Figs 14, 15, Supplementary figs S9, S11); (4) coiled trichomes within the sheath. The closest taxon to *R. halophila* in terms of morphology is *R. biasolettiana*, from which it differs by the presence of granules inside the cells, presence of slime pads, branching pattern, and ecology and geographic distribution (Table 1). According to the original description, *R. biasolettiana* occupies mostly terrestrial habitats in which it is widely distributed, but occasionally may be found in moderately saline waters (Bornet & Flahault, 1888). In contrast, *R. halophila* was collected from the littoral of a hypersaline lake in the Americas in the southern hemisphere (Table 1). *Rivularia bornetiana* (marine) and *R. aquatica* (freshwater) have been reported from Argentina. However, both of these taxa differ from *R. halophila* by having thinner trichomes and differing ecology. *Rivularia dura* and *R. atra* show more or less the same morphology, except that *R. dura* forms only hemispherical and prostrate colonies typically attached to aquatic macrophytes, while *R. atra* forms spherical macrocolonies on stones (Table 1). Ecologically they are very different – *R. atra* is marine in origin and does not precipitate calcium carbonate while *R. dura* occurs in freshwater habitats and precipitates calcium carbonate. Both species are morphologically similar to *R. halophila*, but differ as described above. Additionally, culture material of *R. halophila* was morphologically analogous to *Cyanomargarita melechinii* cultures, mostly in the appearance of cells and the presence of false branching. Nonetheless, *R. halophila* and *C. melechinii* were found to be phylogenetically very distant, and so easily separated (Shalygin *et al.*, 2017).

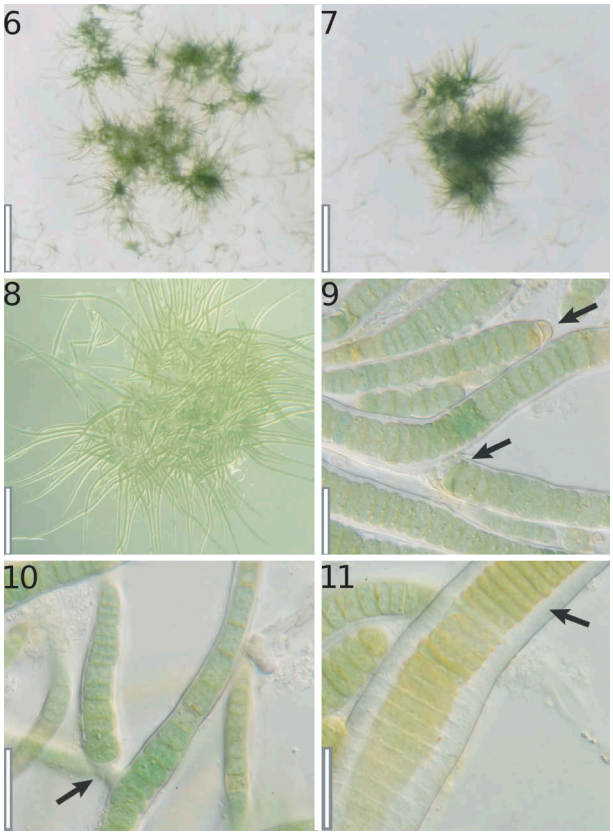

Figs 6–11. Micrographs of *Rivularia halophila* from liquid F/2 medium. **Fig. 6**. Several nearly spherical macroscopic colonies. **Fig. 7**. Almost spherical macroscopic colonies, typical for *Rivularia*. **Fig. 8**. Round colony with filaments spreading out of the centre, in peripheral parts filaments arranged in parallel. **Fig. 9**. Single-false branched filament, with necridic cell (arrow), basal heterocyte also indicated with arrow. **Fig. 10**. *Rivularia*-like type of filament arrangement, with the slime pad (arrow) in the basal part of the short trichome. **Fig. 11**. Mature filament with slightly widened sheath, having perpendicular striations, with meristematic zone (arrow) of the trichome in upper part of figure. Scale bars: Fig. 6 = 2 mm, Fig. 7 = 1 mm, Fig. 8 = 0.2 mm, Fig. 9 = 25 µm, Fig. 10 = 20 µm, Fig. 11 = 15 µm.

16S rRNA phylogeny

Our phylogeny is in general agreement with recent published Nostocales phylogenies, with the exception of the

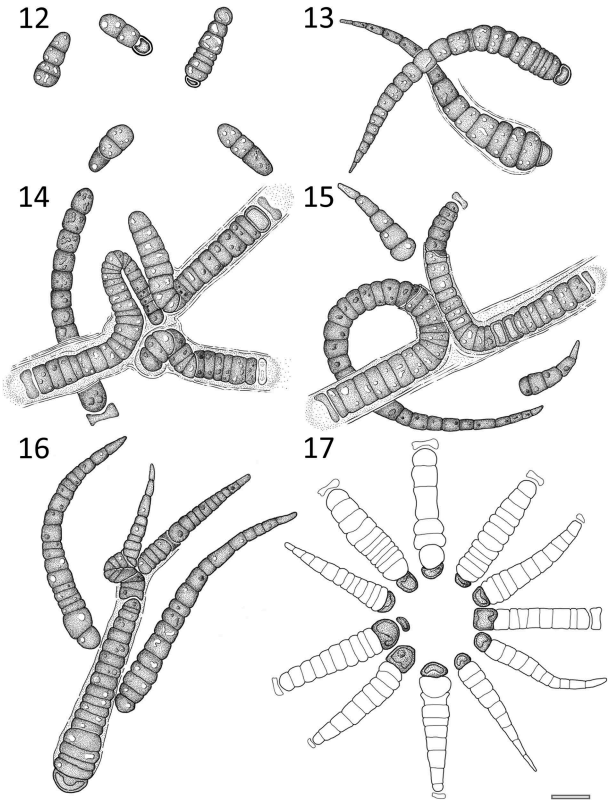

Figs 12–17. Line drawings of *Rivularia halophila* from F/2 culture media. **Fig. 12**. Short hormogonia in juvenile stages. **Fig. 13**. Young sheathless trichome and slightly lamellated filament. **Fig. 14**. Mature, layered filaments with unusual geminate branching, short curved parts (at the middle) possibly represent developing hormogonia. **Fig. 15**. Double-false branching, with tapered filament on the left, released hormogonia. **Fig. 16**. Typical arrangement of the filaments for *Rivularia*. **Fig. 17**. Modelled design of the filaments, bearing variously shaped heterocytes in the basal position. Scale bar = 10 μm.

positioning of Hapalosiphonaceae in the tree (Berrendero Gómez *et al.*, 2016; Oliveira Alvarenga *et al.*, 2016). Moreover, it is in overall congruence with modern taxonomic revisions based on 16S rRNA and protein coding gene sequence data. The deep nodes in our phylogenetic tree represent monophyletic clusters of families and genera, which are consistent with modern nomenclature (Komárek *et al.*, 2014; Shalygin *et al.*, 2017; Mareš, 2018) (See Figs 18–19, Supplementary fig. S3). Topology of the BI tree was similar to that of ML and MP trees, but was better supported at a number of nodes (Supplementary fig. S3). The only clades not congruent among the three analyses were the *Scytonematopsis contorta, Roholtiella* and *Gloeotrichia* clades. However, the *Rivularia* clade was always in the same position. The Rivulariaceae clade, which contains *Rivularia, Kyrtuthrix* and *Nunduva*, is what we consider to be Rivulariaceae *sensu stricto* (Fig. 19). It excludes the clade containing *Calothrix* and *Macrochaete* (Fig. 18). *Phyllonema aviceniicola* has an unstable position. In its original description it was sister to a large clade containing taxa from diverse families, including Rivulariaceae, *Calothrix*, Nostocaceae and Tolypothricaceae (see fig. 1B in Oliveira Alvarenga *et al.*, 2016). In our phylogeny it is sister to the Hapalosiphonaceae, but unsupported. *Phyllonema* was found to be the closest taxon to Rivulariaceae according to the p-distance analysis (Table 2), and was within the Rivulariaceae in the most recently published phylogenetic analysis (González-Resendiz *et al.*, 2018). Clustering together with '*Calothrix*' sp. CCMEE 5093 (AY147029), *R. halophila* forms a clade sister to a brackish *Rivularia* spp. group containing *R. atra*, which is the type species for the genus (Gardner, 1932). *R. halophila* appears taxonomically separate from '*Calothrix*' sp. CCMEE 5093 based on morphology and ecology, even though the two strains have sequences with the moderately high 16S rRNA gene similarity of 99.1% (Table 2). That degree of similarity has been considered to differentiate some species within Nostocales (Vaccarino & Johansen, 2012; Johansen *et al.*, 2014; Kaštovský *et al.*, 2014; Bohunická *et al.*, 2015; Shalygin *et al.*, 2017), although it is above the 98.7% threshold for separation recommended by Yarza *et al.* (2014). Consequently, we would say we lack molecular evidence that the two strains are different species, and that the 16S rRNA similarity is uninformative at this level. Despite the minor morphological similarities between *R. halophila* and '*Calothrix*' sp. CCMEE 5093 (Brenowitz & Castenholz, 1997; Dillon & Castenholz, 2003; Dillon *et al.*, 2003), such as overlapping sheath and morphometric characters, these two morphotypes are drastically different in terms of substrate preference (calcium carbonate versus siliceous rocks), ecological and hydrological preferences (halophilic versus thermotolerant), location (S. America/Andes versus N. America/Yellowstone), and morphology (Table 1). Nevertheless, the taxonomic decision concerning whether these two strains should be considered separate or the same species must be made after the full ITS sequence for '*Calothrix*' sp. CCMEE 5093 becomes available, and a full morphological study of the strain is conducted. Importantly, even without the ITS analysis, it is evident that '*Calothrix*' sp. CCMEE 5093 belongs to the genus *Rivularia*.

ITS structural analysis

We amplified the 16S rRNA gene together with 16S-23S ITS region in one PCR reaction and obtained 4 almost identical clones of *R. halophila* (Boyer *et al.*, 2001; Osorio-Santos *et al.*, 2014; Johansen *et al.*, 2017). After an NCBI blast search for the close relatives of *R. halophila* using the ITS sequence, we could find only five sequences from members of the clade containing *Rivularia, Kyrtuthrix* and *Nunduva* (Figs 20–21). The ITS sequences obtained showed length and sequence heterogeneity, with the shorter sequence corresponding to *R. halophila* – 551 bp, and

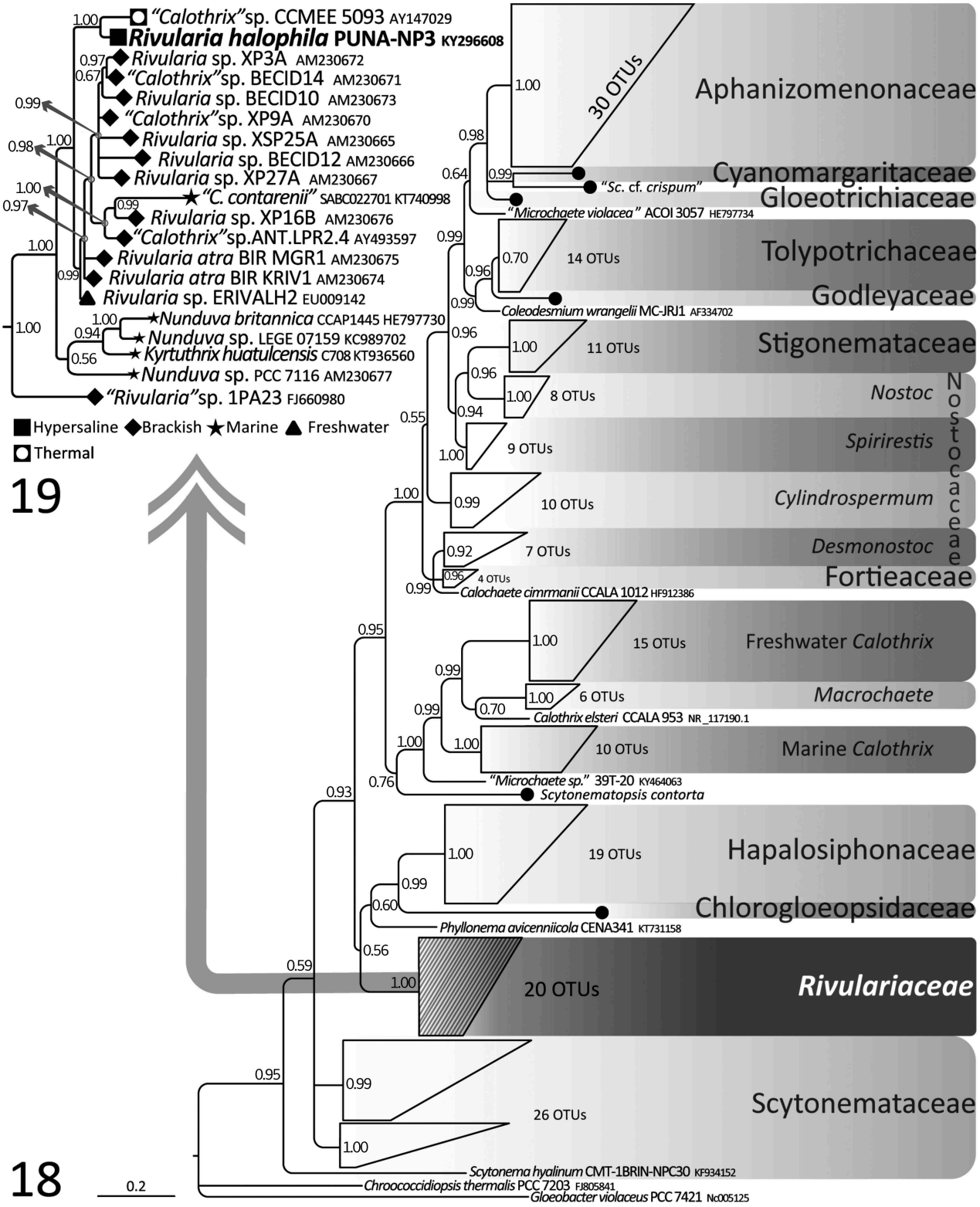

Figs 18–19. Bayesian phylogenetic tree, showing position of the new species of *Rivularia* within Nostocales based on 1496 nucleotides from 16s rRNA gene (209 OTUs). Branch support values are shown as posterior probabilities from the BI analysis (for support values from ML and MP, see Fig. S13). Nodes in the BI analysis are considered strongly supported if the posterior probability exceeds 0.90, weakly supported between 0.80–0.90, and unsupported below 0.80. We report values so that unsupported nodes can be better evaluated by the reader. **Fig. 18**. Full Nostocales tree, with *Rivularia*/*Kyrtuthrix*/*Nunduva* group in dark box above Scytonemataceae; black circles indicate terminal clades. Full phylogeny is available as Supplementary Fig. S13. **Fig. 19**. Uncollapsed part of *Rivularia* tree indicating exact position of *R. halophila* separated from all other *Rivularia* spp.; labels at terminal nodes show different ecological preferences of members of *Rivularia*. Names of the lineages in quotation marks are strains which are misidentified or need to be revised taxonomically.

Table 2. P-distance matrix of Rivulariaceae, including *Rivularia halophila*.

Strains	1	2	3	4	5	6	7	8	9	10	11
1. ***Rivularia halophila* PUNA-NP3 KY296608**											
2. '*Calothrix*' sp. CCMEE5093 AY147029	**99.11**										
3. *Rivularia atra* BIR MGR1 AM230675	**99.11**	98.44									
4. *Rivularia atra* BIR KRIV1 AM230674	**99.11**	98.45	99.56								
5. *Rivularia* sp. XP16B AM230676	**99.00**	98.33	99.34	99.56							
6. *Rivularia* sp. BECID10 AM230673	**98.89**	98.22	99.11	99.34	99.11						
7. *Rivularia* sp. XP3A AM230672	**98.78**	98.11	99.22	99.67	99.45	99.45					
8. *Kyrtuthrix huatulcensis* C708 M11 KT936560	**98.00**	97.31	97.77	98.22	98.11	97.99	98.10				
9. '*Calothrix contarenii*' SABC022701 KT740998	**97.42**	96.85	97.88	98.10	98.10	97.65	97.99	96.61			
10. *Nunduva* sp. PCC7116 AM230677	**96.40**	95.71	96.17	96.63	96.51	96.40	96.51	96.52	94.98		
11. '*Rivularia*' sp. 1PA23 FJ660980	**96.07**	95.37	96.06	96.52	96.29	96.30	96.41	96.64	94.64	95.48	
12. *Phyllonema avicenniicola* CENA341 KT731158	**94.31**	93.59	93.95	94.18	93.83	93.95	93.82	94.09	92.23	92.74	95.12

with the longest sequence belonging to *Nunduva britannica* CCAP1445.1 – 674 bp (González-Resendiz *et al.*, 2018). The ITS region of *N. britannica* is unusually long, probably due to an insertion flanking the D1-D1′ region on 3′ side of the gene (González-Resendiz *et al.*, 2018). Hypothetical secondary structures of the D1-D1′ helix were found to be more or less conservative across all ITS structures in our data set, which was consistent with previous research (Hentschke *et al.*, 2017). The D1-D1′ helix from the available selection of sequences from the *Rivularia* clade exhibits two distinctive morphological motifs (Figs 20–21). Type 1 is represented by *K. huatulcensis* C708 and '*Rivularia*' sp. 1PA23. It differs from the rest by having a single, large terminal loop (with up to 15 bp) and a basal unilateral bulge with sequence 5′–CAUCCC–3′. Type 2 includes *R. halophila*, *N. britannica* CCAP 1445, and *Nunduva* sp. PCC7116 (the latter formerly *Rivularia*, see González-Resendiz *et al.*, 2018), with a 5 bp terminal loop of variable sequence, and an adenine or guanine residue opposite the basal unilateral bulge, which has a sequence of 5′–ACAUCCC–3′. *Nunduva* sp. PCC7116 has a smaller unilateral bulge due to the pairing of the last C with the G on the 5′ strand. The secondary structure of the Box-B helix appears to be more variable in comparison with the D1-D1′ helix and it was almost impossible to identify structural similarities among motifs. Some conservative sequences have been observed, for example, the stable basal clamp (5′–AGCA:UGCU–3′), as well as a region with 5′–AAGU–3′ on the 3′ strand (Fig. 22). The Box-B helix of *R. halophila* was most similar to *N. britannica* CCAP 1445 and *Nunduva* sp. PCC7116, but was shorter. The available V3 helices were all structurally divergent (Fig. 23).

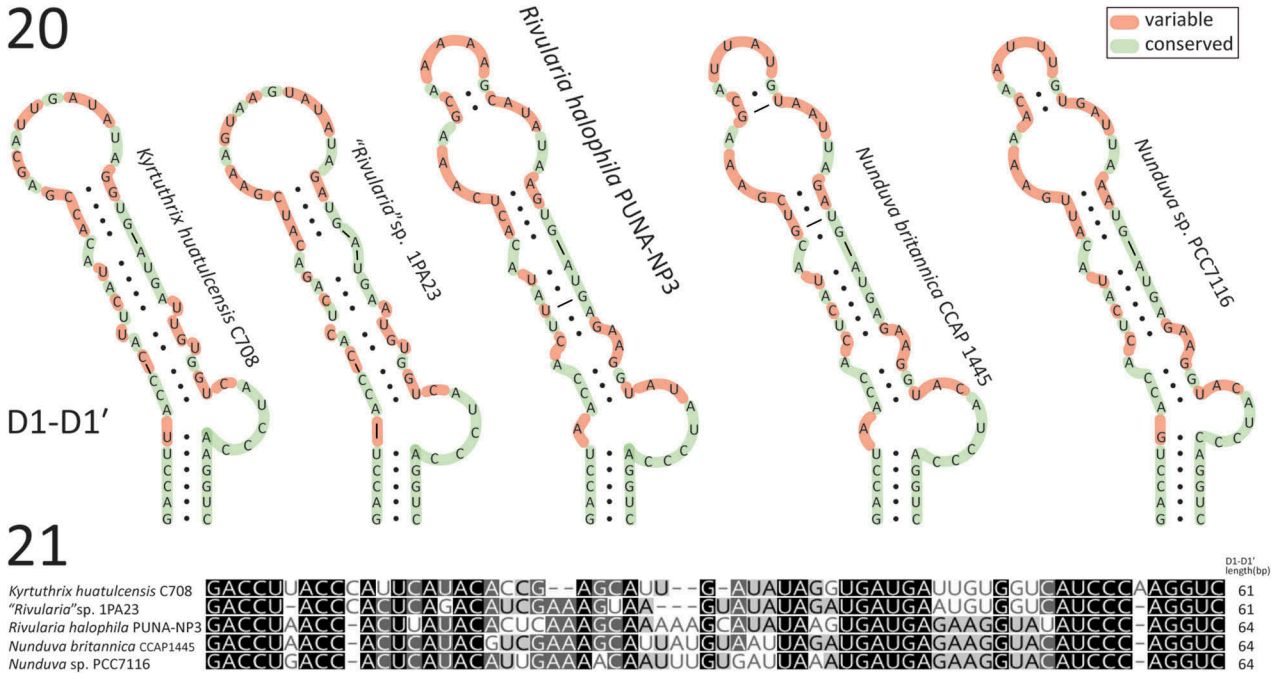

Figs 20–21. Structural differences and dissimilarities in sequences of D1-D1′ region between *R. halophila* and some representatives of Rivulariaceae. **Fig. 20**. Hypothetical secondary structures of D1-D1′ helix with colour codes: pale green represents conservative regions across selected taxa, pale red indicates variable sequences. **Fig. 21**. Geneious alignment of D1-D1′ region, white letters on the black background implies 100% similar sequences within current set of the species. Pale grey letters on the white background indicates lowest similarities. Right column is showing length of D1-D1′.

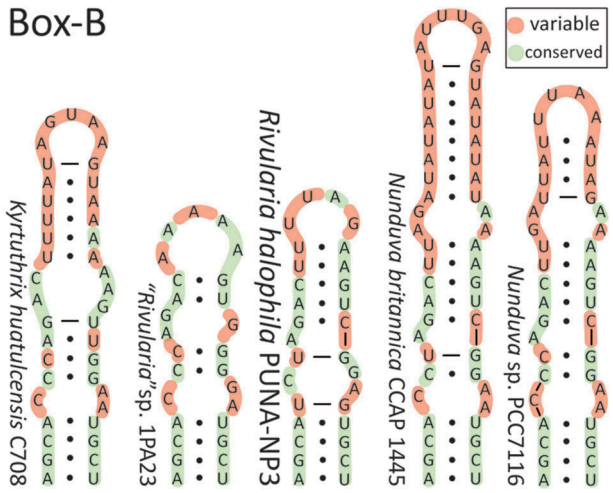

Fig. 22. Predicted secondary structures of Box-B helix from 16S-23S ITS region, colour codes showing differences in aligned sequences: pale red colour represents variable sequences, pale green indicates conservative regions across selected taxa.

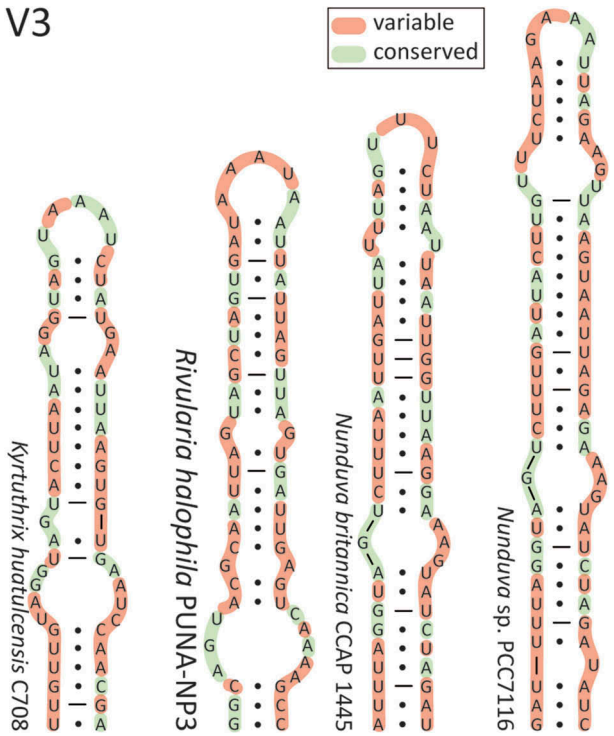

Fig. 23. The most variable region of ITS from Rivulariaceae data set of sequences – V3, same colour codes as shown at the previous figures of ITS.

Discussion

The Rivulariaceae contains taxa which phylogenetically belong in three deep clades, which will probably be recognized at the family level. *Gloeotrichia* has already been separated into its own family, the Gloeotrichaceae (Komárek *et al.*, 2014). More intensively sampled phylogenies also suggest that the clade containing *Calothrix* and *Macrochaete* is deeply separated from the clade containing *Phyllonema, Rivularia*, *Kyrtuthrix* and *Nunduva* (González-Resendiz *et al.*, 2018). There is taxonomic work remaining in both putative families, with many undetermined species having been isolated and sequenced, but the family-level clades are phylogenetically stable when a sufficiently large taxon sample is used.

In the past 10 years, a number of cyanobacterial taxa have been described, mostly using a combination of 16S rRNA and sometimes multilocus phylogenies with additional information from morphological observations (Hentschke *et al.*, 2016; Rigonato *et al.*, 2016; Sciuto & Moro, 2016; Zimba *et al.*, 2017). However, as previously discussed by many authors (Komárek, 2013; Komárek *et al.*, 2014; Berrendero Gómez *et al.*, 2016; Shalygin *et al.*, 2017), only a few address higher hierarchical taxonomic groups, e.g. families or higher. Some of the newly established taxa have *incertae familiae* status, such as *Scytonematopsis contorta* and *Aetokthonos hydrillicola* (Vaccarino & Johansen, 2011; Wilde *et al.*, 2014). *Scytonematopsis contorta*, for example, belongs to Scytonemataceae according to Komárek *et al.* (2014), but has an unstable position outside the clade containing *Scytonema sensu stricto* in the phylogenies published to date (Bohunická *et al.*, 2015; Berrendero Gómez *et al.*, 2016). *Aetokthonos hydrillicola* was assigned to Hapalosiphonaceae in Komárek *et al.* (2014) due to its ability to form true branches. However, recent phylogenies showed *A. hydrillicola* to be far outside the Hapalosiphonaceae, closer to the Nostocaceae (Saber *et al.*, 2017). The clade containing *Aetokthonos* may be an independent true branching lineage (Wilde *et al.*, 2014), and most likely it should belong to its own family.

In the case of the Rivulariaceae, sequence data for the type species of *Rivularia*, i.e. the type genus of the family, were available as *Rivularia atra* BIR MGR1 (AM230675), a potential reference strain for the type species, but the morphological characterization of this strain is not available and it was not isolated from the type locality. *Rivularia halophila* was placed phylogenetically in the Rivulariaceae clade with high support (Figs 18–19; Supplementary fig. S3). In addition, *R. halophila* expressed the typical morphology for the genus in many traits including the appearance of macroscopic colonies in both natural populations and in culture, the arrangement of the filaments, and the tapering of trichomes. Based on the combination of several lines of evidence we describe *R. halophila* as a new species in the genus *Rivularia* within Rivulariaceae. In addition, according to the principle of monophyly, *Macrochaete* and *Calothrix* probably belong in a family separate from the Rivulariaceae (Komárek *et al.*, 2014; Berrendero Gómez *et al.*, 2016; Shalygin *et al.*, 2017).

Acknowledgements

We thank the Department of Plant and Environmental Sciences (NMSU) in general and Pietrasiak Lab in particular for hosting the senior author. Stephanie Willette kindly provided us with F/2 media. Additional thanks to the anonymous reviewer who provided constructive suggestions which have improved the manuscript in many ways.

Disclosure statement

No potential conflict of interest was reported by the authors.

Funding

This research was completed with the support of the following projects: International cooperation program: CONICET-CNRS (Le Centre National de la Recherche Scientifique (Paris, France, Res. 730/15). 'Microbial carbonate precipitation in hypersaline lakes: microbe-mineral interactions in extreme environments and their implication for CO_2 storage in carbonates', and CONICET-PIP-2015-2017. Johansen received support from a grant from the Grant Agency of the Czech Republic, P506/15–11912S.

Supplementary information

The following supplementary material is accessible via the Supplementary Content tab on the article's online page at http://doi.org/10.1080/09670262.2018.1479887
Supplementary figs S1–6. Micrographs of *R. halophila* from solid Z8 media. **Fig. S1**. Macroscopic colonies; scale bar represents 1 mm. **Fig. S2**. Isopolar trichomes tapered to both ends, attached to the long lamellated main filaments; scale bar represents 150 µm. **Fig. S3**. *Tapinothrix clintonii*-like trichomes; scale bar represents 40 µm. **Fig. S4**. Young, U-shaped, isopolar trichome, and geminate branched trichome (arrow); scale bar represents 40 µm. **Fig. S5**. Star-like fascicle, with filaments spreading from the centre, scale bar represents 35 µm. **Fig. S6**. Empty, sheath from mature filament, with the parallel striation perpendicular to the main axes; scale bar represents 35 µm.
Supplementary figs S7–12. Line drawings of *R. halophila* from Z8 media. **Fig. S7**. Hormogonia; scale bar represents 10 µm. **Fig. S8**. Young heteropolar trichomes without sheaths; scale bar represents 10 µm. **Fig. S9**. Single-false branched filament above, and two heteropolar filaments derived from geminate branching below; scale bar represents 10 µm. **Fig. S10**. Long, mature, unbranched filaments with necridic cells and widened lamellations; scale bar represents 20 µm. **Fig. S11**. Double-false branched filament on the left, and two trichomes inside of sheaths as well as coiled trichome; scale bar represents 20 µm. **Fig. S12**. Massive nodule with coiled trichomes within, with heteropolar filaments extending outside the sheath material; scale bar represents 20 µm.
Supplementary fig. S13. Uncollapsed phylogenetic tree for Rivulariaceae inside Nostocales inferred by BI Analysis from the 16S rRNA gene. Support values are shown as BI/ML/MP. Support values of 100 in ML and MP, or 1.00 (BI), are displayed as '*', nodes with support less that 50 (ML, MP) or 0.5 (BI) are shown as '-', respectively.

Author contributions

S. Shalygin: original concept, drafting and editing manuscript, analysis of molecular data, graphical design, reviewing process; N. Pietrasiak: original concept, drafting and editing manuscript, isolation of the culture, performing molecular methods; F. Gomez: drafting and editing manuscript, sampling of the mat, sample site characterization, pictures for Figs 1-5; C. Mlewski: drafting and editing manuscript, sampling of the mat, sample site characterization, confocal microscopy; E. Gerard: confocal microscopy; J. Johansen: drafting and editing manuscript, reviewing process.

ORCID

Sergei Shalygin http://orcid.org/0000-0001-8886-6666

References

Berrendero Gómez, E., Johansen, J.R., Kaštovský, J., Bohunická, M. & Čapková, K. (2016). *Macrochaete* gen. nov. (Nostocales, Cyanobacteria), a taxon morphologically and molecularly distinct from *Calothrix*. *Journal of Phycology*, **52**: 638–655.

Bohunická, M., Pietrasiak, N., Johansen, J.R., Gómez, E.B., Hauer, T., Gaysina, L.A. & Lukešová, A. (2015). *Roholtiella*, gen. nov. (Nostocales, Cyanobacteria) – a tapering and branching cyanobacteria of the family Nostocaceae. *Phytotaxa*, **197**: 84–103.

Bornet, E. & Flahault, C. (1888). *Revision des Nostocacées hétérocystées Contenues dans les Principaux Herbiers de France*. Annales des Sciences Naturelles, Botanique, Septième Série 7.

Boyer, S.L., Flechtner, V.R. & Johansen, J.R. (2001). Is the 16S-23S rRNA internal transcribed spacer region a good tool for use in molecular systematics and population genetics? A case study in cyanobacteria. *Molecular Biology and Evolution*, **18**: 1057–1069.

Brandes, M., Albach, D.C., Vogt, J.C., Mayland-Quellhorst, E., Mendieta-Leiva, G., Golubic, S. & Palinska, K.A. (2015). Supratidal extremophiles—cyanobacterial diversity in the rock pools of the Croatian Adria. *Microbial Ecology*, **70**: 876–888.

Brenowitz, S. & Castenholz, R.W. (1997). Long-term effects of UV and visible irradiance on natural populations of a scytonemin-containing cyanobacterium (*Calothrix* sp.). *FEMS Microbiology Ecology*, **24**: 343–352.

Countway, P.D., Gast, R.J., Savai, P. & Caron, D.A. (2005). Protistan diversity estimates based on 18S rDNA from seawater incubation in the Western North Atlantic. *Journal of Eukaryotic Microbiology*, **52**: 95–106.

Darriba, D., Taboada, G.L., Doallo, R. & Posada, D. (2012). jModelTest 2: more models, new heuristics and parallel computing. *Nature Methods*, **9**: 772.

Davydov, D. (2017). Cyanoprokaryotes of the west part of Oscar II Land, West Spitsbergen Island, Spitsbergen archipelago. *Czech Polar Reports*, **7**: 94–108.

Dillon, J.G. & Castenholz, R.W. (2003). The synthesis of the UV-screening pigment, scytonemin, and photosynthetic performance in isolates from closely related natural populations of cyanobacteria (*Calothrix* sp.). *Environmental Microbiology*, **5**: 484–491.

Dillon, J.G., Miller, S.R. & Castenholz, R.W. (2003). UV-acclimation responses in natural populations of

cyanobacteria (*Calothrix* sp.). *Environmental Microbiology*, **5**: 473–483.

Domínguez-Escobar, J., Beltrán, Y., Bergman, B., Díez, B., Ininbergs, K., Souza, V. & Falcón, L.I. (2011). Phylogenetic and molecular clock inferences of cyanobacterial strains within Rivulariaceae from distant environments. *FEMS Microbiology Letters*, **316**: 90–99.

Drummond, A.J., Ho, S.Y.W., Phillips, M.J. & Rambaut, A. (2006). Relaxed phylogenetics and dating with confidence. *PLoS Biology*, 4: e88.

Elenkin, A.A. (1938). *Monographia algarum cyanophycearum aquidulcium et terrestrium in finibus URSS inventarum. (Sinezelenye vodorosli SSSR)*. Izd. AN SSSR, Moskva-Leningrad.

Gardner, N.L. (1932). The Myxophyceae of Porto Rico and the Virgin Islands. In Scientific Survey of Porto Rico and the Virgin Islands, Volume III, Part 2, 249–311 (+2 plates). New York Academy of Sciences, New York.

Geitler, L. (1932). *Cyanophyce*. In *Kryptogamen-Flora von Deutschland* (Rabenhorst, L., editor). Koeltz Scientific Books, Koenigsteim.

Geitler, L. (1942). Schizophyta: Klasse Schizophyceae. In *Die Natürlichen Pflanzenfamilien nebst ihren Gattungen und wichtigeren Arten, insbesondere den Nutzpflanzen unter Mitwirkung zahlreicher hervorragender Fachgelehrten Begrundet von A. Engler und K. Prantl* (Harms, H. & Mattfeld, J., editors). Wilhelm Engelmann, Leipzig.

Gelman, A. & Rubin, D.B. (1992). Inference from iterative simulation using multiple sequences. *Statistical Science*, **7**: 457–511.

Gérard, E., Ménez, B., Couradeau, E., Moreira, D., Benzerara, K., Tavera, R. & López-García, P. (2013). Specific carbonate–microbe interactions in the modern microbialites of Lake Alchichica (Mexico). *ISME Journal*, **7**: 1997–2009.

Golubic, S. (1973). The relationship between blue-green algae and carbonate deposits. In *The Biology of Blue-Green Algae* (Carr, N.G. & Whitton, B.A., editors), 434–472. Basil Blackwell, Oxford.

Golubic, S. & Campbell, S.E. (1981). Biogenically formed aragonite concretions in marine *Rivularia*. In *Phanerozoic Stromatolites* (Monty, C., editor), 209–229. Springer, Berlin.

Gomez, F.J., Kah, L.C., Bartley, J.K. & Astini, R.A. (2014). Microbialites in a high-altitude Andean lake: multiple controls on carbonate precipitation and lamina accretion. *Palaios*, **29**: 233–249.

González-Resendiz, L., Johansen, J.R., Alba-Lois, L., Segal-Kischinevzky, C., Escobar-Sánchez, V., Jimenez-Garcia, L. F., Hauer, T. & León-Tejara, H. (2018). *Nunduva*, a new marine genus of Rivulariaceae (Nostocales, Cyanobacteria) from marine rocky shores. *Fottea*, **18**: 86–105

Guillard, R.R.L. & Ryther, J.H. (1962). Studies of marine planktonic diatoms: I. *Cyclotella nana* Hustedt, and *Detonula confervacea* (Cleve) Gran. *Canadian Journal of Microbiology*, **8**: 229–239.

Guiry, M.D. & Guiry, G.M. (2017). *AlgaeBase*. National University of Ireland, Galway. http://www.algaebase.org.

Hentschke, G.S., Johansen, J.R., Pietrasiak, N., Fiore, M. F., Rigonato, J., Anna, C.L.S. & Komárek, J. (2016). Phylogenetic placement of *Dapisostemon* gen. nov. and *Streptostemon*, two tropical heterocytous genera (Cyanobacteria). *Phytotaxa*, **245**: 129–143.

Hentschke, G., Johansen, J.R., Pietrasiak, N., Rigonato, J., Fiore, M.F. & Leite Sant'Anna, C. (2017). *Komarekiella atlantica* gen. et sp. nov. (Nostocaceae, Cyanobacteria): a new subaerial taxon from the Atlantic Rainforest and Kauai, Hawaii. *Fottea*, **17**: 178–190.

Hindák, F. (2007). Conspicuous forms of heterocytes and hormogonia in *Rivularia mesenterica* (Cyanophyta/Cyanobacteria). *Phytologia*, **13**: 21–27.

Johansen, J.R. & Casamatta, D. (2005). Recognizing cyanobacterial diversity through adoption of a new species paradigm. *Archiv fur Hydrobiologie. Supplementband: Algological Studies*, **117**: 71–93.

Johansen, J.R., Bohunická, M., Lukešová, A., Hrčková, K., Vaccarino, M.A. & Chesarino, N.M. (2014). Morphological and molecular characterization within 26 strains of the genus *Cylindrospermum* (Nostocaceae, Cyanobacteria), with descriptions of three new species. *Journal of Phycology*, **50**: 187–202.

Johansen, J.R., Mareš, J., Pietrasiak, N., Bohunická, M., Zima, J., Štenclová, L. & Hauer, T. (2017). Highly divergent 16S rRNA sequences in ribosomal operons of *Scytonema hyalinum* (Cyanobacteria). *PLoS ONE*, **12**: 1–16.

Kaštovský, J., Berrendero Gómez, E., Hladil, J. & Johansen, J.R. (2014). *Cyanocohniella calida* gen. *et* sp. nov. (Cyanobacteria: Aphanizomenonaceae) a new cyanobacterium from the thermal springs from Karlovy Vary, Czech Republic. *Phytotaxa*, **181**: 279–292.

Kearse, M., Moir, R., Wilson, A., Stones-Havas, S., Cheung, M., Sturrock, S., Buxton, S., Cooper, A., Markowitz, S., Duran, C., Thierer, T., Ashton, B., Meintjes, P. & Drummond, A. (2012). Geneious Basic: an integrated and extendable desktop software platform for the organization and analysis of sequence data. *Bioinformatics*, **28**: 1647–1649.

Komárek, J. (2013). *Cyanoprokaryota – 3. Teil/Part3: Heterocytous genera (Süßwasserflora von Mitteleuropa Bd. 19/3)*. Springer, Heidelberg.

Komárek, J., Kaštovský, J., Mareš, J. & Johansen, J.R. (2014). Taxonomic classification of cyanoprokaryotes (cyanobacterial genera) 2014, using a polyphasic approach. *Preslia*, **86**: 295–335.

Kotai, J. (1972). Instructions for preparation of modified nutrient solution Z8 for algae. *Norwegian Institute for Water Research*, **11**: 5.

Kumar, S., Stecher, G. & Tamura, K. (2016). MEGA7: Molecular Evolutionary Genetics Analysis Version 7.0 for bigger datasets. *Molecular Biology and Evolution*, **33**: 1870–1874.

León-Tejera, H., González-Resendiz, L., Johansen, J.R., Segal-Kischinevzky, C., Escobar-Sánchez, V. & Alba-Lois, L. (2016). Phylogenetic position reevaluation of *Kyrtuthrix* and description of a new species *K. huatulcensis* from Mexico's Pacific coast. *Phytotaxa*, **278**: 1–18.

Mareš, J. (2018). Multilocus and SSU rRNA gene phylogenetic analyses of available cyanobacterial genomes, and their relation to the current taxonomic system. *Hydrobiologia*, **811**: 19–34.

Melechin, A.V., Dadydov, D.A. Shalygin, S.S. & Borovichev, E.A. (2013). Open informational system on biodiversity of cyanoprokaryotes and lichens – CRIS (Cryptogamic Russian Information System). *Bulletin MOIP*, **9**: 51–56. [In Russian]

Merz-Preiß, M. & Riding, R. (1999). Cyanobacterial tufa calcification in two freshwater streams: ambient environment, chemical thresholds and biological processes. *Sedimentary Geology*, **126**: 103–124.

Miller, M., Schwartz, T., Pickett, B., He, S., Klem, E., Scheuermann, R., Passarotti, M., Kaufman, S. &

O'Leary, M. (2015). A RESTful API for Access to Phylogenetic Tools via the CIPRES Science Gateway. *Evolutionary Bioinformatics*, **11**: 43–48.

Obenlüneschloss, J. & Schneider, J. (1991). Ecology and calcification patterns of *Rivularia* (Cyanobacteria). *Archiv fur Hydrobiologie. Supplementband: Algological Studies*, **64**: 489–502.

Oliveira Alvarenga, D., Rigonato, J., Zanini Branco, L.H., Melo, I.S. & Fiore, F.M. (2016). *Phyllonema aviceniicola* gen. nov., sp. nov. and *Foliisarcina bertiogensis* gen. nov., sp. nov., epiphyllic cyanobacteria associated with *Avicennia schaueriana* leaves. *International Journal of Systematic and Evolutionary Microbiology*, **66**: 689–700.

Oren, A. (2015). Cyanobacteria in hypersaline environments: biodiversity and physiological properties. *Biodiversity and Conservation*, **24**: 781–798.

Osorio-Santos, K., Pietrasiak, N., Bohunická, M., Miscoe, L.H., Kováčik, L., Martin, M.P. & Johansen, J.R. (2014). Seven new species of *Oculatella* (Pseudanabaenales, Cyanobacteria): taxonomically recognizing cryptic diversification. *European Journal of Phycology*, **49**: 450–470.

Pentecost, A. (1988). Growth and calcification of the cyanobacterium *Homoeothrix crustacea*. *Journal of General Microbiology*, **134**: 2665–2672.

Perkerson III, R.B., Johansen, J.R., Kovácik, L., Brand, J., Kaštovský, J. & Casamatta, D.A. (2011). A unique Pseudanabaenalean (Cyanobacteria) genus *Nodosilinea* gen. nov. based on morphological and molecular data. *Journal of Phycology*, **47**: 1397–1412.

Perona, E. & Mateo, P. (2006). Benthic cyanobacterial assemblages as indicators of nutrient enrichment regimes in a Spanish river. *Acta Hydrochimica et Hydrobiologica*, **34**: 67–72.

Řeháková, K., Johansen, J.R., Bowen, M.B., Martin, M.P. & Sheil, C.A. (2014). Variation in secondary structure of the 16s rRNA molecule in cyanobacteria with implications for phylogenetic analysis. *Fottea*, **14**: 161–178.

Rigonato, J., Gama, W.A., Oliveira Alvarenga, D., Zanini Branco, L.H., Brandini, F.P., Genuário, D.B. & Fiore, M. F. (2016). *Aliterella atlantica* gen. nov., sp. nov., and *Aliterella antarctica* sp. nov., novel members of coccoid Cyanobacteria. *International Journal of Systematic and Evolutionary Microbiology*, **66**: 2853–2861.

Ronquist, F., Teslenko, M., Van Der Mark, P., Ayres, D. L., Darling, A., Höhna, S., Larget, B. Liu, L., Suchard, M.A. & Huelsenbeck, J.P. (2012). MrBayes 3.2: Efficient Bayesian phylogenetic inference and model choice across a large model space. *Systematic Biology*, **61**: 539–542.

Saber, A.A., Cantonati, M., Mareš, J., Anesi, A. & Guella, G. (2017). Polyphasic characterization of *Westiellopsis prolifica* (Hapalosiphonaceae, Cyanobacteria) from the El-Farafra Oasis (Western Desert, Egypt). *Phycologia*, **56**: 697–709.

Sciuto, K. & Moro, I. (2016). Detection of the new cosmopolitan genus *Thermoleptolyngbya* (Cyanobacteria, Leptolyngbyaceae) using the 16S rRNA gene and 16S–23S ITS region. *Molecular Phylogenetics and Evolution*, **105**: 15–35.

Shalygin, S. (2012). Epilithic and epiphytic cyanoprokaryota from Lapland Biosphere Reserve. PhD dissertation. [In Russian]

Shalygin, S., Shalygina, R., Johansen, J.R., Pietrasiak, N., Berrendero Gómez, E., Bohunická, M., Mareš, J. & Sheil, C.A. (2017). *Cyanomargarita* gen. nov. (Nostocales, Cyanobacteria): convergent evolution resulting in a cryptic genus. *Journal of Phycology*, **53**: 762–777.

Sihvonen, L.M., Lyra, C., Fewer, D.P., Rajaniemi-Wacklin, P., Lehtimäki, J.M., Wahlsten, M. & Sivonen, K. (2007). Strains of the cyanobacterial genera *Calothrix* and *Rivularia* isolated from the Baltic Sea display cryptic diversity and are distantly related to *Gloeotrichia* and *Tolypothrix*. *FEMS Microbiology Ecology*, **61**: 74–84.

Stamatakis, A., Hoover, P. & Rougemont, J. (2008). A rapid bootstrap algorithm for the RAxML Web servers. *Systematic Biology*, **57**: 758–571.

Swofford, D.L. (2002). PAUP*. *Phylogenetic analysis using parsimony (* and other methods). Version 4*. Sinauer Associates, Sunderland, MA.

Vaccarino, M.A. & Johansen, J.R. (2011). *Scytonematopsis contorta* sp. nov. (Nostocales), a new species from the Hawaiian Islands. *Fottea*, **11**: 149–161.

Vaccarino, M.A. & Johansen, J.R. (2012). *Brasilonema angustatum* sp. nov. (Nostocales), a new filamentous cyanobacterial species from the Hawaiian Islands. *Journal of Phycology*, **48**: 1178–1186.

Vondrášková, A., Fibich, P., Lepš, J. & Kaštovský, J. (2017). Determinants of cyanobacterial species composition in the splash zone of two Croatian islands. *European Journal of Phycology*, **52**: 179–187.

Wilde, S.B., Johansen, J.R., Wilde, H.D., Jiang, P., Bartelme, B. & Haynie, R.S. (2014). *Aetokthonos hydrillicola* gen. *et* sp. nov.: epiphytic cyanobacteria on invasive aquatic plants implicated in avian vacuolar myelinopathy. *Phytotaxa*, **181**: 243–260.

Yarza, P., Yilmaz, P., Pruesse, E., Glöckner, F.O., Ludwig, W., Schleifer, K.-H., Whitman, W.B., Euzéby, J., Rudolf, A. & Rosselló-Móra, R. (2014). Uniting the classification of cultured and uncultured bacteria and archaea using 16S rRNA gene sequences. *Nature Reviews Microbiology*, **12**: 635–645.

Zimba, P.V., Huang, I.-S., Foley, J.E. & Linton, E.W. (2017). Identification of a new-to-science cyanobacterium, *Toxifilum mysidocida* gen. nov. & sp. nov. (Cyanobacteria, Cyanophyceae). *Journal of Phycology*, **53**: 188–197.

Zuker, M. (2003). Mfold web server for nucleic acid folding and hybridization prediction. *Nucleic Acids Research*, **31**: 3406–3415.